



HAL
open science

Study of water vapor vertical variability and possible cloud formation with a small network of GPS stations

Joël van Baelen, Guillaume Penide

► **To cite this version:**

Joël van Baelen, Guillaume Penide. Study of water vapor vertical variability and possible cloud formation with a small network of GPS stations. *Geophysical Research Letters*, 2009, 36 (2), pp.n/a-n/a. 10.1029/2008GL036148 . hal-02092540

HAL Id: hal-02092540

<https://uca.hal.science/hal-02092540>

Submitted on 5 Aug 2021

HAL is a multi-disciplinary open access archive for the deposit and dissemination of scientific research documents, whether they are published or not. The documents may come from teaching and research institutions in France or abroad, or from public or private research centers.

L'archive ouverte pluridisciplinaire **HAL**, est destinée au dépôt et à la diffusion de documents scientifiques de niveau recherche, publiés ou non, émanant des établissements d'enseignement et de recherche français ou étrangers, des laboratoires publics ou privés.

Copyright

Study of water vapor vertical variability and possible cloud formation with a small network of GPS stations

Joël Van Baelen¹ and Guillaume Penide¹

Received 26 September 2008; revised 3 December 2008; accepted 5 December 2008; published 17 January 2009.

[1] During a short experiment we have investigated the vertical variability of water vapor in the lower part of the atmosphere with the help of small network of GPS stations positioned on the eastern slopes of the Puy de Dôme in central France. We have found out that the urban layer exhibits somewhat constant water vapor content. In contrast, the major IWV variations arise in the upper troposphere level, in particular in the presence of westerly flows that bring elevated water vapor content over the mountain ridge. Finally, the transition layer situated between these lower and upper levels presents quite variable water vapor content, acting as a buffer zone for the boundary layer. Comparing two episodes of higher water vapor contents, one being associated with a sharp frontal passage, we have shown that the contrasted behavior of the different layers revealed the possible formation of clouds before the advent of rain. **Citation:** Van Baelen, J., and G. Penide (2009), Study of water vapor vertical variability and possible cloud formation with a small network of GPS stations, *Geophys. Res. Lett.*, 36, L02804, doi:10.1029/2008GL036148.

1. Introduction

[2] It has now been largely established that, beyond precise positioning and navigation applications, Global Positioning Systems (GPS) are also adequate tools to monitor the atmospheric water vapor [Bevis *et al.*, 1992, 1994; Businger *et al.*, 1996; Duan *et al.*, 1996; Tregoning *et al.*, 1998; Wolfe and Gutman, 2000].

[3] The Zenith Tropospheric Delay (ZTD) parameter derived by GPS network analysis software, such as GAMIT in our case [King and Bock, 2000], and the knowledge of the surface pressure and temperature at the GPS sites enable accurate retrieval of the Integrated Water Vapor (IWV) above the corresponding GPS stations. This quantity, usually expressed in millimeters [mm], corresponds to the height of liquid water one would obtain if all the water vapor available in the atmospheric column directly above the station was condensed. It is often determined with an equation such as [Van Baelen *et al.*, 2005]:

$$IWV = \frac{10^5}{461.51 \times \left[\frac{k_3}{(a_0 + a_1 \times T_S)} + (k_2 - 0.622 \times k_1) \right]} \times \left[ZTD - \frac{2.9349 \cdot 10^{-5} \times k_1 \times P_s}{(1 - 0.00266 \times \cos(2\Psi) - 0.00028 \times H)} \right]$$

where ZTD is the GPS observable, H and Ψ are the altitude and latitude of the GPS station respectively, P_s and T_S are the

¹Laboratoire de Météorologie Physique, Université Blaise Pascal Clermont-Ferrand II, CNRS, Aubière, France.

surface pressure and temperature respectively, and k_1 , k_2 , k_3 , a_0 and a_1 are coefficients linked to the atmospheric refractive index [Boudouris, 1963; Saastamoinen, 1972; Thayer, 1974] and to the estimation of the atmospheric mean temperature from the surface temperature with an empirical model [Bevis *et al.*, 1994; Emardson and Derks, 1999].

[4] Times series of GPS derived IWV's have been the object of many studies for the sake of validation against other means of water vapor measurements such as radiosoundings, microwave radiometers, lidars, etc. [Liljegren *et al.*, 1999; Niell *et al.*, 2001; Van Baelen *et al.*, 2005] as well as against models [Guerova *et al.*, 2003]. Likewise, IWV's from GPS networks have been used to provide 2-D maps of water vapor and study the time evolution of water vapor distribution in the framework of numerous case studies [Champollion *et al.*, 2004; Walpersdorf *et al.*, 2004], while punctual studies using temporary dense networks of GPS stations have addressed water vapor tomography for 3-D water vapor field retrieval [Champollion *et al.*, 2005]. Furthermore, work has been carried out recently to provide global estimates of water vapor using existing long term GPS data sets [Wang *et al.*, 2007], while national weather services start assimilation of GPS water vapor products [Gutman *et al.*, 2004].

[5] However, little attention has been devoted so far to the vertical variability of water vapor using a limited number of GPS estimates of IWV and their continuous and high time resolution capabilities. Such a study is the object of the work presented here.

2. Puy de Dôme Experiment

[6] In order to investigate the vertical variability of water vapor we designed a small experiment that benefited from the local topography of the Clermont-Ferrand area. The city lies at the foothill of the "Chaîne des Puys" mountain ridge with a very nearby summit about 1000 meters above the city (Puy de Dôme 1465m). Thus, we installed three temporary GPS stations in different instrumented sites managed by our laboratory that included both pressure and temperature measurements and such that their corresponding altitudes covered the entire range. The first site (OPGC, altitude 423m) was on the university campus close to the city, the second site (OPME, altitude 657 m) was located at the wind profiler radar site near Opme on a small plateau between the campus and the Puy de Dôme, and finally the third site (PDOM, altitude 1447 m) was on top of Puy de Dôme. The corresponding experimental layout is illustrated in Figure 1 which also provides the corresponding altitude and horizontal spacing of the stations. Hence, one can easily identify various atmospheric layers: the total atmospheric column above OPGC, the lower urban layer between OPGC and OPME (layer 1), a transition layer between OPME and PDOM (layer 2), and the "free" troposphere above PDOM.

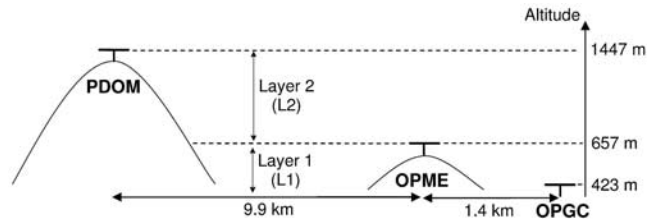


Figure 1. Layout of the experimental setup.

[7] The corresponding GPS data of the three stations were processed together with an ensemble of 10 reference stations for network analysis using the GAMIT software [King and Bock, 2000]. The methodology used to retrieve the ZTD estimates follows the one described by Walpersdorf *et al.* [2004]: a first analysis with little constraints on the experiment temporary station coordinates, then a positioning solution through Kalman filtering applied on the entire network, and finally a second analysis with high coordinate constraints and a sliding window strategy in order to determine the tropospheric parameters (namely, the ZTD's) with a 1 hour time resolution. Once the ZTD time series were calculated for all the stations over the entire period of the experiment, they were converted to IWV using the formula expressed above with the pressure and temperature measurements obtained at each site and averaged over a duration corresponding to the GPS solution time interval of one hour.

3. General Study

[8] Figure 2 shows the IWV contents of the different atmospheric layers for the entire period of the experiment and supports the preliminary discussions. Overall, one can notice that the total column IWV above OPGC (the lowest station, upper dotted curve) and PDOM (the highest station, upper solid curve) present very similar features both in relative amplitude and in time. Thus, the corresponding features of the atmospheric layer between OPGC and PDOM (i.e., L1 + L2, the layer below 1447 meters, solid thick curve) are much more “damped”. Also, the marked increases of total water vapor content observed in the individual IWV time series are missing while the contribution of the OPGC to PDOM layer is somewhat equivalent to the IWV contribution above PDOM. This indicates that during the length of our experiment the IWV variability arises predominantly within the troposphere region above the mountain ridge, according to the varying synoptic conditions we have encountered, while the L1 + L2 layer corresponds somewhat, although not strictly, to the moist atmospheric boundary layer. Second, the urban boundary layer (L1, lower solid curve) exhibits fairly constant water vapor content and is the largest water vapor contributor below PDOM while it accounts for only one fourth of the thickness (234 m out of 1024m). Finally, the transition layer (L2, lower dotted curve) shows a water vapor content slightly less than the underlying urban layer with sometimes very low values, usually, but not exclusively, when the total IWV is low. The above statements will be looked into details in the light of the following case studies. However, there is one more point that needs further comments. There are times when the L2 IWV value (OPME – PDOM) becomes negative. That is of course not physically correct but those instances are always quite limited in time. Hence, one could argue that it is still within the admitted

accuracy of GPS IWV retrieval of about 1 mm. We also noticed that these situations arose mainly when there was a temperature inversion above OPGC. In these cases, the negative IWV difference would be linked to an erroneous approximation of the mean temperature (T_m) based on the measured surface temperature (T_s) [Bevis *et al.*, 1994]. But this correlation is not always verified, so there should still be another explanation to the negative IWV differences. Furthermore, we have found that it was associated with cases when the ZWD from PDOM (thus even before transformation into IWV via $T_m(T_s)$) was very similar or, at times, slightly superior to the one of OPME, thus leading to negative IWV for the concerned layer. The most probable explanation is therefore the geographical separation between the stations and, thus, the influence of IWV gradients in the total water vapor while the transition layer is extremely dry. That is certainly the case in cold winter days when the major contribution to the water vapor is brought by a higher altitude westerly flow passing over the mountains.

[9] Another aspect of our study that we have approached qualitatively already is the variability of the water vapor content in the various layers of the atmosphere. We have seen above that the urban boundary layer seemed quite stable, while there was enhanced variability in the upper layers. That is summarized in Figure 3 where one can see the water vapor content relative variability (as the ratio in % of standard deviation over mean value) for each layer and/or group of layers for the entire period of the experiment. When one compares the total column (OPGC) with the layer above the mountain range (PDOM), it appears that there is a higher variability in the layer PDOM than under. This finding confirms that the water vapor modifications are predominantly influenced by the large scale meteorological conditions which in this case are the synoptic structures passing above the orography. Within the lower layers between OPGC and PDOM, the lowest urban layer (L1) is obviously very stable when compared to the transition layer (L2) where the lowest IWV content and the highest variability is found. It appears as if the L2 layer plays a role of buffer between the atmospheric urban layer and the free troposphere above. That is further demonstrated by the observation (Figures 2 and 4) that the

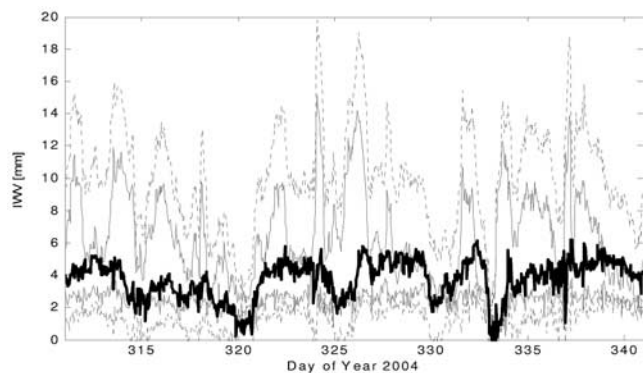


Figure 2. Time series of GPS retrieved IWV over the entire length of the experiment (days 311 to 341) for OPGC (upper dotted curve) and PDOM (upper solid curve) total columns, and for lower layers: the urban layer (OPGC-OPME, L1, lower solid curve), the transition layer (OPME-PDOM, L2, lower dotted curve) and the OPGC-PDOM layer (L1 + L2, thick solid curve).

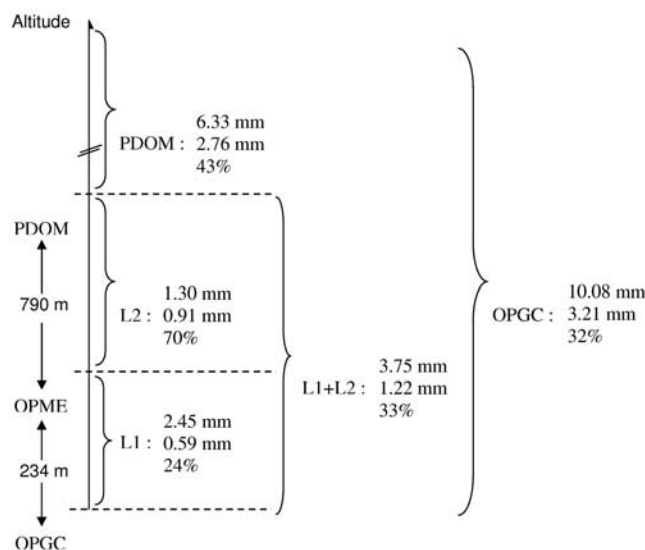


Figure 3. Variability of the water vapor content in the different layers: respectively the mean IWV, the standard deviation and relative variation (ratio of standard deviation to mean value) of IWV.

L2 variations often appears in opposite phase with the slight variations of the boundary layer. This can be explained if one considers that the actual urban layer with somewhat constant water vapor content can expand and “spill over” from L1 into the L2 transition layer above, or in the contrary contract into a layer of thickness equal or less than the one of the L1 layer.

4. Case studies

[10] We will now focus on the two major IWV peaks that occurred on days 324 and 326. Figure 4 offers a close up of the corresponding IWV time series for the same layers as in Figure 2. An arrow on Figure 4 indicates the time of strong but short lived precipitations recorded at the OPGC site.

[11] The first episode on day 324 is associated with a north westerly flow and high wind velocities corresponding to a frontal passage that brings humidity from the Atlantic Ocean over the mountain ridge. This episode is made up of three separate phases. First, there is a marked rise of the total IWV above the stations. It is rather rapid with about 10 mm increases over all sites (OPGC and PDOM being represented here) in the lapse of two to three hours. One can notice that the water vapor content in the lower layers does not show much variation over that same period of time. Thus, the IWV increase is the fact of the upper layer only, above the Puy de Dôme level.

[12] Then, there is a slow decrease of the total IWV between 2:00 and 9:00 UTC while during that time the water vapor content actually increases in the lower layers. The later fact is further confirmed by sharp mixing ratio increases recorded both at OPGC and OPME right at the time of the strong IWV decrease associated with precipitations. This indicates that the water vapor brought above the mountain ridge has moved past the Puy de Dôme slopes over the Clermont-Ferrand basin. The water vapor content rises mainly in the transition layer L2 and “fills up” the lower levels above the lowest urban layer L1. However, this new vertical distribution of water vapor should not affect the total IWV which

should globally still be increasing. So why does it decrease? Our proposed hypothesis is that there is formation (or development) of clouds above the Puy de Dôme, as the liquid water droplets formed by water vapor condensation become invisible to the GPS. That hypothesis is further supported by the sustained ascending vertical velocities measured by the wind profiler at Opme exhibiting more than 3 m/s between 2.5 and 7 km of altitude, and by the strong conditional instability of the atmosphere at that time. Thus, two processes take place: in the lower levels the water vapor sinks into the Clermont-Ferrand valley, while aloft the saturated moist air is lifted such that condensation arises and water vapor is transformed into hydrometeors within the developing cloud. The final stage of the event corresponds to the actual passage of the front, when temperature decreases and pressure rises again after reaching a minimum. That time is associated with a short but intense rain episode that takes place at 9:00. It is also associated with a marked decrease of IWV as the atmosphere above is no longer the source of higher water vapor contents while the precipitation also depletes the layers below the cloud level of its water vapor.

[13] The second episode on days 325 and 326 does not correspond to a frontal passage above the stations although it is still associated with a north westerly flow but much less intense than in the previous days. In this case, the episode exhibits only two phases. First there is a slow IWV rise when increased water vapor contents are brought up by the N-W flow above the mountain ridge. The IWV peak value is reached at PDOM (on top of the mountain ridge) before OPGC (in the valley below to the East). During that time, the lower layers water vapor content keeps constant at first then it increases, mainly in the transition layer L2, as the water vapor fills the entire column. For the second phase of the event, the decrease of IWV is similarly slow and, given the lower layers water vapor content keeps steady, one can assume it is due to a drying upper level atmosphere without the formation of clouds.

5. Preliminary Conclusions and Perspectives

[14] In this short study we have considered the vertical variability of water vapor estimated with a small network of temporary GPS stations.

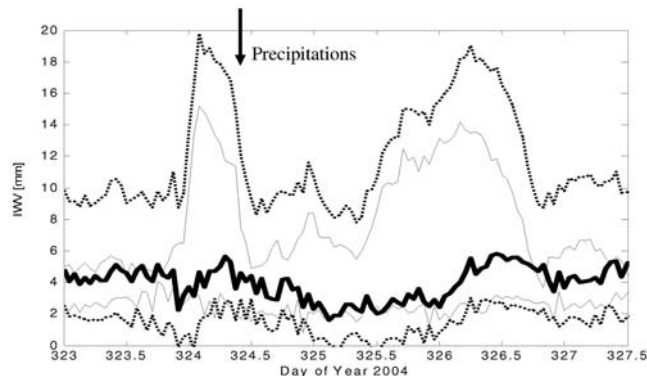


Figure 4. Same as Figure 2 but for a subset of the data including the two significant events analyzed between 18 November 2004 at 00:00 and 22 November 2004 at 12:00. Approximate time of precipitation onset is indicated by the arrow.

[15] Considering the entire length of the experiment, we have noticed that the atmosphere was structured into three different and contrasted layers. First, there is the urban layer (L1) which exhibits fairly constant water vapor content and, although it is less than 250 meters thick, accounts for at least half the water vapor present below the Puy de Dôme which rises 1000 meters above the city floor. Then, the transition layer (L2) between the lowest urban layer (L1) and the top of the Puy de Dôme can show two kinds of behavior. Either it acts as some kind of buffer zone into or from which the atmospheric boundary layer expands or contracts while the water vapor content of these two layers evolves in opposite phases, or it is an intermediate layer when the water vapor brought up above the mountain ridge sinks into the city basin. Finally, during the time of our experiment, most of the large variations of water vapor contents proved to originate in the upper layer, mainly when water vapor is brought over the Puy de Dôme by westerly flows from the Atlantic Ocean. The more detailed study of two episodes of higher IWV have revealed a contrasted behavior in the case of a frontal passage. In such conditions, the slow total IWV decrease associated with the local IWV increase in the lowest atmospheric layers before the onset of rain is the probable signature of cloud formation.

[16] The work presented here is preliminary in the sense that it covers only a short period of time and a reduced number of meteorological conditions. Thus, this calls for follow up studies through the establishment of a permanent set of stations for continuous measurements such that various meteorological regimes can be considered. In particular, it would be of great interest to study the moist boundary layer evolution during summer periods when the diurnal cycle of evaporation can play a major role through surface release of water vapor. Furthermore, events of intense precipitations could be observed in conjunction with the newly acquired observatory precipitation radar in order to investigate the role of IWV variations in the various atmospheric layers as a precursor of such events. Thus, to pursue our investigations, we hope for a slightly larger network with extra stations extending our investigations to the city and eastern plains floor some tens of meters below the campus, as well as in the interval between OPME and PDOM. Likewise, short campaigns with a dense network of GPS stations around the established ones can be envisioned to study the 3-D water vapor distribution and dynamics with tomography studies.

[17] **Acknowledgments.** The authors would like to acknowledge the support of the Observatoire de Physique du Globe de Clermont-Ferrand (OPGC) and, in particular, the dedicated assistance of Jean-Marc Pichon during the measurement campaign. The temporary GPS stations were provided by the INSU instrumentation park. Finally, the authors want to thank Bob King and Paul Tregoning for their numerous advice and support regarding GAMIT processing and for thoughtful discussions.

References

- Bevis, M., S. Businger, T. A. Herring, C. Rocken, R. A. Anthes, and R. H. Ware (1992), GPS meteorology: Remote sensing of atmospheric water vapor using the Global Positioning System, *J. Geophys. Res.*, *103*, 15,787–15,801.
- Bevis, M., S. Businger, S. Chiswell, T. A. Herring, R. A. Anthes, C. Rocken, and R. H. Ware (1994), GPS meteorology: Mapping zenith wet delays onto precipitable water, *J. Appl. Meteorol.*, *33*, 379–386.
- Boudouris, G. (1963), On the index of refraction of air, the absorption and dispersion of centimeter waves by gases, *J. Res. Natl. Bur. Stand. U.S., Sect. D*, *67*, 631–684.
- Businger, S., S. R. Chiswell, M. Bevis, J. Duan, R. A. Anthes, C. Rocken, H. Ware, M. Exner, T. VanHove, and F. Solheim (1996), The promise of GPS in atmospheric monitoring, *Bull. Am. Meteorol. Soc.*, *77*, 5–18.
- Champollion, C., F. Masson, J. Van Baelen, A. Walpersdorf, J. Chéry, and E. Doerflinger (2004), GPS monitoring of the tropospheric water vapor distribution and variation during the 9 September 2002 torrential precipitation episode in the Cévennes (southern France), *J. Geophys. Res.*, *109*, D24102, doi:10.1029/2004JD004897.
- Champollion, C., F. Masson, M.-N. Bouin, A. Walpersdorf, E. Doerflinger, O. Bock, and J. Van Baelen (2005), GPS water vapor tomography: First results from the ESCOMPTE field experiment, *Atmos. Res.*, *74*, 253–274.
- Duan, J., et al. (1996), GPS Meteorology: Direct estimation of the absolute value of precipitable water, *J. Appl. Meteorol.*, *35*, 830–838.
- Emardson, T. R., and H. J. P. Derks (1999), On the relation between the wet delay and the integrated precipitable water vapour in the European atmosphere, *Meteorol. Appl.*, *6*, 1–12.
- Guerova, G., E. Brockmann, J. Quiby, F. Schubiger, and C. Matzler (2003), Validation of NWP mesoscale models with Swiss GPS network AGNES, *J. Appl. Meteorol.*, *42*, 141–150.
- Gutman, S., S. R. Sahn, S. G. Benjamin, B. E. Schwartz, K. L. Holub, J. Q. Stewart, and T. L. Smith (2004), Rapid retrieval and assimilation of ground based GPS precipitable water observations at the NOAA Forecast Systems Laboratory: Impact on weather forecasts, *J. Meteorol. Soc. Jpn.*, *82*, 351–360.
- King, R. W., and Y. Bock (2000), Documentation for the GAMIT GPS analysis software, release 10.0, Mass. Inst. of Technol, Cambridge.
- Liljegren, J., B. Lesht, T. VanHove, and C. Rocken (1999), A comparison of integrated water vapor from microwave radiometer, balloon-borne sounding system and global positioning system, paper presented at the Ninth ARM Science Team Meeting, U.S. Dep. of Energy, San Antonio, Tex., 22–26 March.
- Niell, A. E., A. J. Coster, F. S. Solheim, V. B. Mendes, A. Toor, R. B. Langley, and C. A. Upham (2001), Comparison of measurements of atmospheric wet delay by radiosonde, water vapour radiometer, GPS, and VLBI, *J. Atmos. Oceanic Technol.*, *18*, 830–850.
- Saastomoinen, J. (1972), Atmospheric correction for the troposphere and stratosphere in radio ranging of satellites, in *The Use of Artificial Satellites for Geodesy*, *Geophys. Monogr. Ser.*, vol. 15, edited by S. W. Henriksen et al., pp. 247–251, AGU, Washington, D. C.
- Thayer, G. D. (1974), An improved equation for the radio refractive index of air, *Radio Sci.*, *9*, 803–807.
- Tregoning, P., R. Boers, D. O'Brien, and M. Hendy (1998), Accuracy of absolute precipitable water vapor estimates from GPS observations, *J. Geophys. Res.*, *103*, 28,701–28,710.
- Van Baelen, J., J.-P. Aubagnac, and A. Dabas (2005), Comparison of near real-time estimates of integrated water vapor derived with GPS, radiosondes, and microwave radiometer, *J. Atmos. Oceanic Technol.*, *22*, 201–210.
- Walpersdorf, A., O. Boch, E. Doerflinger, F. Masson, J. VanBaelen, A. Somieski, and B. Bürki (2004), Data analysis of a dense GPS network operated during the ESCOMPTE campaign, *Phys. Chem. Earth*, *29*, 201–211.
- Wang, J., L. Zhang, A. Dai, T. Van Hove, and J. Van Baelen (2007), A near-global, 2-hourly data set of atmospheric precipitable water from ground-based GPS measurements, *J. Geophys. Res.*, *112*, D11107, doi:10.1029/2006JD007529.
- Wolfe, D. E., and S. I. Gutman (2000), Developing and operational surface-based GPS water vapor observing system for NOAA: Network design and results, *J. Atmos. Oceanic Technol.*, *17*, 426–440.

G. Penide and J. Van Baelen, Laboratoire de Météorologie Physique, Université Blaise Pascal Clermont-Ferrand II, CNRS, 24 Avenue des Landais, F-63177 Aubière, CEDEX, France. (j.vanbaelen@opgc.univ-bpclermont.fr)